All-Spray-Coated Inverted Semitransparent Organic Solar Cells and Modules

Yu-Ching Huang, Cheng-Wei Chou, De-Han Lu, Charn-Ying Chen, and Cheng-Si Tsao

***Abstract*—The aim of this study is to demonstrate a fabrication process of all-sprayed inverted organic photovoltaics. We sprayed the blend of poly(3-hexylthiophene-2,5-diyl) and [6,6]phenyl-C_{61}-butyric acid methyl ester as an active layer and zinc oxide prepared by a sol–gel process as an electron transport layer. The highly conductive poly(3,4-ethylenedioxythiophene):poly(styrenesulfonate) as a semitransparent anode and alternative to Ag is sequentially spray-coated. We further utilize nitrogen (N_2) plasma modification on the active layer for improving the compatibility between two layers in this work. With a combination of tuning the subsequent thermal treatment, the all-sprayed devices with good performance could be obtained. The highest power conversion efficiency (PCE) of 2.90% is achieved by optimizing the N_2 plasma and thermal treatment, and the stability test is performed. Moreover, we upscaled the all-spray-coating process to a module with three cells connected in series, and the PCE of the module is achieved to 2.44%.**

***Index Terms*—Module, organic photovoltaic (OPV), plasma modification, semitransparent, spray coating.**

I. Introduction

SIGNIFICANT improvements in power conversion efficiency (PCE) of the organic photovoltaics (OPVs) have been achieved in recent years [1]–[4]. With the aid of its impressive PCE, many research works have been conducted to develop the mass production of OPVs with the unique advantage of processing, which is feasible to large-area solution-processed manufacture on flexible substrates [5]–[7]. Among the current technologies suitable for mass production, the spray process has been extensively investigated as a promising candidate to replace the spin process commonly used in laboratories. The spray process emerged as a cost-effective manufacture of large-area OPVs due to its high throughput rate and low materials waste [6], [8], [9]. In particular, the spray process is a well-established technology in the industry. It is easy to deposit various layers on substrates with the tunable topologies. The PCE of spray-coated OPVs is limited by the series resistance (R_s) resulting from the droplet boundary in sprayed films. Previous studies have proposed many methods to eliminate the droplet boundary, such as multisource deposition [10], solvent treatment over layer deposition [11], and hot solvent vapor annealing [6]. Most of the related literature focus on how to reduce the intraresistance within the droplet boundary in the single spray-coated layer; however, the research investigating the inter-resistance from the interfacial contact between each spray-coated layers stacked in the OPV is still lacking.

Operation lifetime of devices is also an important factor in the commercialization of OPVs. An inverted architecture is demonstrated to effectively improve the operating lifetime of OPVs. In comparison with the conventional architecture, n-type metal oxides as an electron transport layer (ETL) are deposited on top of an indium tin oxide (ITO) transparent electrode instead of poly(3,4 ethylenedioxylenethiophene):poly(styrene sulfonic acid) (PEDOT:PSS) [12]. Many studies have pointed out that etching of ITO by the acidic PEDOT:PSS is the major cause of the PCE degradation of conventional OPVs. In addition, high work-function metals, such as silver (Ag) and gold (Au), as anodes in the inverted architecture can exhibit a much better oxidation resistance as compared with an Al electrode used in the conventional OPVs. However, these Ag or Au electrodes are usually deposited by using a thermal evaporation under vacuum process. The processing step of evaporated metal layers restricts the high throughput goal of OPVs. It is noteworthy that one of the key advantages of OPVs is the rapid energy payback time [13], an alternative solution-processed electrode to the thermally evaporated electrode could effectively reduce the energy payback time. An all-solution-coated process, including the top electrodes (such as high-conductivity PEDOT:PSS and Ag nanowires), has been proposed to easily fabricate the large-area OPVs or roll-to-roll OPV modules toward commercialization [14]–[18]. Moreover, applying such top electrodes enables the manufacture of semitransparent OPVs due to their tunable transparency. Among the current processing techniques of the all-solution-processed semitransparent OPV, the PEDOT:PSS anode has the very cost-effective advantage compared to the metal anodes (such as Ca, Ag, Au), or transparent oxide anodes, which are excessively reactive or expensive [15], [16]. Generally, the solution-processed anode would lower the PCE. The interface between spray-coated photoactive layer and electrodes plays an important role in controlling charge transport and collection. For solving this problem, the literature [15] about the transparent anode added dimethyl sulfoxide into PEDOT:PSS solution to improve the wetness on the active layer. To date, the study of how to improve the interfacial interaction or morphology to enhance the PCE of fully spray-coated OPVs is still limited. It shows

Manuscript received September 29, 2017; accepted October 13, 2017. Date of publication November 2, 2017; date of current version December 20, 2017. *(Corresponding author: Yu-Ching Huang.)*

The authors are with the Institute of Nuclear Energy Research, Taoyaun 32546, Taiwan (e-mail: huangyc@iner.gov.tw; cwchou@iner.gov.tw; ldhjay@iner.gov.tw; cychen@iner.gov.tw; cstsao@iner.gov.tw).

Color versions of one or more of the figures in this paper are available online at http://ieeexplore.ieee.org.

Digital Object Identifier 10.1109/JPHOTOV.2017.2764143

the challenge of solving the problems from the contact or interlayer (usually PEDOT:PSS) between active layer and semitransparent electrode. Kang *et al*. prepared all-sprayed-coated devices based on the structure of ITO/zinc oxide (ZnO)/ poly(3-hexylthiophene-2,5-diyl) (P3HT):[6,6]phenyl-C_{61}-butyric acid methyl ester (PCBM)/poly(3,4-ethylenedioxythiophene):poly(styrenesulfonate) (PH1000) with a PCE of 2.53% [15]. Kim *et al.* prepared all-spin-coated devices based on the architecture of ITO/ZnO/ P3HT:PCBM/PEDOT:PSS/PH1000 with a PCE of 2.49% [19]. Ding *et al*. prepared a device with a structure of ITO/ZnO/P3HT:PCBM/PEDOT:PSS/PH1000:Ag nanowire that presented a PCE of 2.1% [20].

Generally speaking about OPVs, the challenge remains to transfer the high PCE obtained on laboratory-scale devices to the large-area module. The efforts of large-area processing for large cells and modules have been presented [21]–[23]. Recently, there is a remarkable progress in the PCE of spray-coated OPVs presented in the literature due to the use of novel polymers [8], [24]–[27]. The highest PCE of ∼9% of spray-coated OPVs could be achieved. Because the solution deposition adopted for chemical modification for interface has the problem of nonuniformity and can be easily influenced by the other synthesis factors, it may lead to the large PCE reduction when the device is scaled up to large-area module. In contrast, the plasma modification has the superiority of good uniformity, simplicity, and stability, leading the superiority of fabrication of large-area module.

Very few successful OPV studies using radiation or plasma modification were reported. The main cause is the structural defects (atomic or molecular scale) caused by the excitation and ionization from the incident nitrogen ions (as heavy charged particles here). The positive effect on the surface modification brought by a plasma technique is usually reduced or offset due to the produced structural defects in materials [28], [29]. Fortunately, on the other hand, the structural defects produced during plasma irradiation may be concurrently reduced in number or recovered by the thermal diffusion and recombination of charges or ions (self-curing). Moreover, the thermal annealing treatment adopted effectively to reduce the structural defects caused by the radiation is frequently reported in the other fields or materials (thermal curing) [28], [29]. These factors (ionization rate by high-energy nitrogen ions, self-curing at room temperature, and thermal curing) complicate the plasma damage effect when the degree of constructive surface modification is proportional to the total plasma amounts.

In this present study, we applied the highly conductive PEDOT:PSS (named as PH1000) as a semitransparent top electrode to develop the fully spray-coated inverted OPVs. The PH1000 layer also served as the hole transport layer (HTL) for reducing the fabrication steps. The PH1000 anode has to be spray-coated on the photoactive layer, which is usually prepared with hydrophobic organic solvent. The compatibility between PH1000 anode and active layer is poor due to the hydrophilic nature of PEDOT:PSS. The poor compatibility resulted in a poor interfacial contact and thus decreased the PCE of fully spray-coated OPVs. We provide a facile method to improve the compatibility between hydrophobic photoactive layer and hydrophilic PEDOT:PSS anode by nitrogen (N_2) plasma modification on the active layer. The effect of plasma treatment on 1) the interfacial contact between spray-coated layers and semitransparent PH1000 anode, 2) the induced degradation to the active layer, and 3) enhancement of device performance is systematically discussed here. The PCE of the fully spray-coated semitransparent OPV with the device area of 1 cm × 0.3 cm can be achieved to 2.90% by enhancement of plasma modification in contrast to that of the reference device with MoO_3/Ag anode (2.92%). We also upscale such a semitransparent plasma-treated fully spray-coated OPV to the module comprising three cells in series with the cell area of 1 cm × 4 cm. The effect of plasma treatment on the stability of the semitransparent fully spray-coated OPVs is presented. These results could provide sufficient information for developing the commercial fabrication and evaluation of the transparent all-spray-coated OPVs with the PEDOT:PSS anode from the cell to module scale.

II. Experimental Details

A. Materials

P3HT was purchased from Rieke metals. PCBM was supplied from Nano-C and highly conductive PEDOT:PSS (CleviosTM PH1000) was from Heraeus. Other chemicals and solvents were purchased from Sigma-Aldrich, and used as received.

B. ZnO Layer Deposited by a Spray Process

To prepare the ZnO precursor solution, we dissolved 21.95 mg of zinc acetate ($Zn(OAc)_2$) and 6.11 mg of monoethanolamine in 1 ml of 2-methoxyethanol. Prior to the spray deposition of ETL, the ITO glass was ultrasonically cleaned in a series of organic solvents (methanol, acetone, and isopropanol), and then treated with O_2 plasma for 3 min. The ZnO ETL was spray-coated under ambient conditions using the ExactCoat system equipped with an AccuMist 120 kHz ultrasonic atomizing nozzle (Sono-Tek Corpoation). ZnO precursor was sprayed on a cleaned ITO glass with a flow rate of $0.2\,\mathrm{ml}\cdot\mathrm{min}^{-1}$, spray speed of $40\,\mathrm{mm}\cdot\mathrm{s}^{-1}$, and 10 cm height from the ITO substrate. The spray-coated ZnO precursor layer was calcined at 150 °C for 60 min in an oven, and the film thickness of ZnO was ∼50 nm.

C. Devices Fabrication and Characterization

In this present study, the inverted device structure of the ITO glass/ZnO/P3HT:PCBM/PEDOT:PSS anode was fabricated. The active layer and PEDOT:PSS top electrode were deposited by the spray-coating process. The thermally evaporated MoO_3/Ag anode was used for a reference OPV device. A mixture solution of P3HT and PCBM (mass ratio = 1:1) dissolving in chlorobenzene with a concentration of $10\,\mathrm{mg}\cdot\mathrm{ml}^{-1}$ was prepared and then stirred at 600 r/min for overnight. The blend solution was spray-coated onto the ZnO layer with a flow rate of $0.15\,\mathrm{ml}\cdot\mathrm{min}^{-1}$, spray speed of $50\,\mathrm{mm}\cdot\mathrm{s}^{-1}$, and 5 cm height from the substrate for three cycles spray deposition. The photoactive layer was thermal annealing at 130 °C for 10 min under ambient environment, and the film thickness is ∼200 nm. Prior

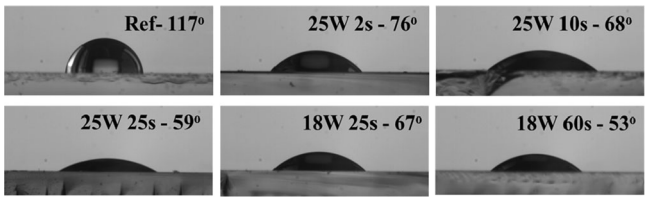

Fig. 1. Contact angles between PH1000 solution drop and the P3HT:PCBM films treated with the plasma treatments of 18 W and 25 W, respectively, for various times.

to a spray-coated PEDOT:PSS anode, the P3HT:PCBM layer was modified by N_2 plasma with the powers of 18 and 25 W, respectively, for various periods. After the plasma modification, PH1000 was spray-coated onto the photoactive layer at flow rate of 0.5 ml $\cdot$ min^{-1}, spray speed of 25 mm $\cdot$ s^{-1}, and 10 cm height from substrate for 20 cycles spray deposition. The sprayed PEDOT:PSS (PH1000) anodes were thermally treated at 100 °C for 10 min (under the ambient condition) into a dry film with a thickness of 2 μm. Different thicknesses of PH1000 anodes were also prepared for the transmittance measurement. The areas of cell devices, defined by the area of anode, were 1 cm $\times$ 0.3 cm for the basic device and 1 cm $\times$ 4 cm for the unit cell of module, respectively. The details of fabrication of series module were described elsewhere [30]. Current–voltage characteristics were measured by using a solar simulator (Abet technologies, Model #11000) under AM 1.5 illumination (100 mW $\cdot$ cm^{-2}) under ambient condition. The sprayed film thicknesses were measured by a profilometer (Alpha Step D-100, KLA Tencor).

III. Result and Discussion

A. N_2 Plasma Effect on P3HT:PCBM Active Layer and PCE Improvement

At first, we demonstrate the effect of N_2 plasma on 1) the surface characteristics of the spray-coated photoactive layer and 2) the degradation of device performance purely caused by the plasma-modified photoactive layer under the plasma power of 25 and 18 W for various treatment times of 2, 10, 25, and 60 s. Fig. 1 shows the contact angles between PH1000 solution drop and the P3HT:PCBM films treated with various plasma modifications. The contact angle of the P3HT:PCBM film without plasma modification is 117° due to the hydrophobicity of the organic photoactive layer. With increasing the N_2 plasma power and treated duration, the contact angles decrease initially with a dramatic drop, indicating that the plasma modification tuned by power and duration can improve the surface wettability between the hydrophobic photoactive layer and hydrophilic PH1000 layer. However, the N_2 plasma modification would simultaneously damage the photoactive layer. One of the main bottlenecks in improving PCE is ascribed to the trade-off between photoactive-layer damage and interfacial contact improvement. Therefore, it is necessary to determine the optimal plasma modification conditions on the photoactive layer, including the plasma power and treated time.

We measured the photovoltaic performance of the degraded devices purely caused by the plasma-modified active layers.

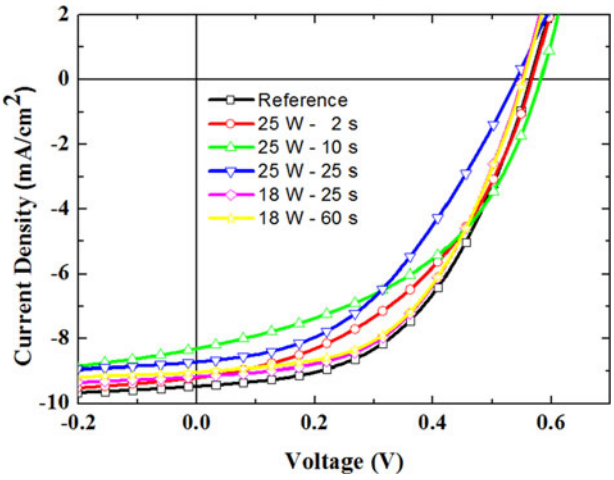

Fig. 2. Voltage–current characteristics of the devices (device area = 1 cm $\times$ 0.3 cm) with the evaporated MoO_3/Ag anode and the spray-coated active layers treated with the plasma power of 1) 25 W for 0 (reference cell; without plasma) 2, 10, and 25 s, and 2) 18 W for 25 and 60 s, respectively.

TABLE I
Photovoltaic Performance Corresponding to Fig. 2 (These Data are Averaged Over Ten Devices Per Processing Condition)

Plasma condition	J_{sc} (mA·cm^{-2})	V_{oc} (V)	FF	PCE (%)
w/o	9.13 ± 0.31	0.56 ± 0.01	51.20 ± 0.9	2.61 ± 0.10
25 W/2 s	9.08 ± 0.10	0.57 ± 0.01	44.28 ± 1.2	2.27 ± 0.07
25 W/10 s	8.24 ± 0.12	0.58 ± 0.01	45.15 ± 0.9	2.14 ± 0.11
25 W/25 s	8.85 ± 0.20	0.54 ± 0.01	40.08 ± 3.4	1.91 ± 0.13
18 W/25 s	9.19 ± 0.27	0.55 ± 0.07	50.78 ± 1.7	2.57 ± 0.05
18 W/60 s	9.12 ± 0.18	0.55 ± 0.01	50.07 ± 3.1	2.53 ± 0.10

These devices are prepared based on the plasma-modified spray-coated photoactive layer with the evaporated MoO_3/Ag top electrode. In this study, the PCE of OPVs was averaged over ten devices for each plasma condition before the evaporation deposition of the MoO_3/Ag electrode. The *J–V* curves are shown in Fig. 2. The corresponding device performances are listed in Table I. For the devices based on the spray-coated photoactive layer modified with a high plasma power of 25 W for 0 (as a reference device), 2, 10, and 25 s, the PCE of a device with N_2 plasma modification of 2 s was reduced from 2.61% (reference device) to 2.27%. The reduction in PCE mainly resulted from the decreasing fill factor (from 51.20% to 44.28%). The decrease of fill factor implies that an increasing surface recombination occurred on the photoactive layer. We further increased the plasma-treated time to 10 and up to 25 s. The PCE of the corresponding devices further decreased to 2.14% and 1.91%, respectively, due to the continuously decreasing fill factor. The longer the plasma-modified time, the lower the fill factor of the devices. These results reveal the negative effect of high N_2 plasma power treatment on the spray-coated photoactive layer, decreasing the PCE of such inverted OPVs. In contrast, the devices modified with a low N_2 plasma power of 18 W for 25 s demonstrated a slightly decreased efficiency (2.57%) as compared with the reference devices (2.61%). Additionally, the device modified with a plasma power of 18 W for a longer time,

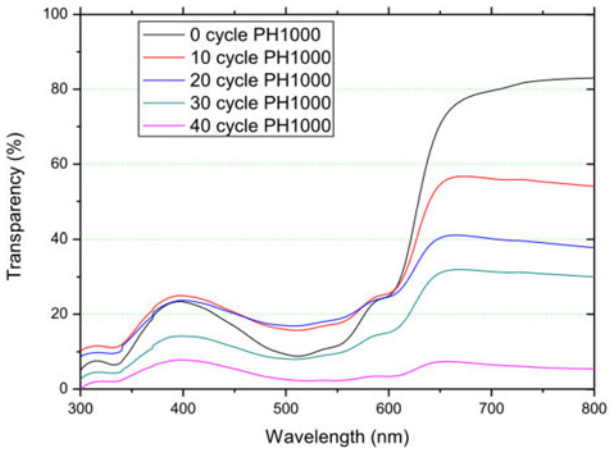

Fig. 3. Transmittance curves corresponding to different thicknesses of PH1000 anodes expressed by the spray cycle number. (The thickness increases with spray cycle number.)

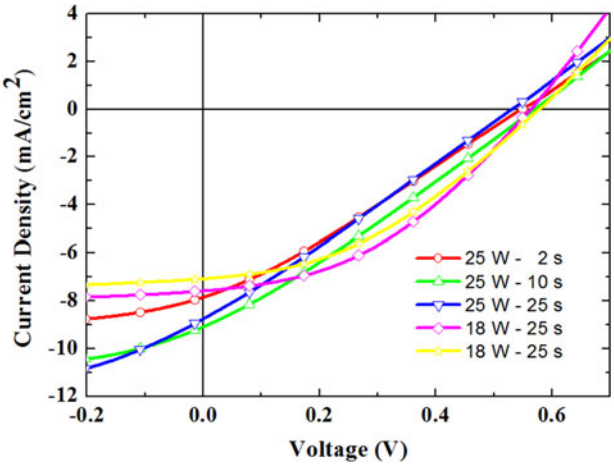

Fig. 4. Voltage–current characteristics of the fully coated semitransparent devices (device area = 1 cm × 0.3 cm) with the active layers treated with 1) 25 W of plasma for 2, 10, and 25 s, and 2) 18 W of plasma for 25 and 60 s.

TABLE II
PHOTOVOLTAIC PERFORMANCE CORRESPONDING TO FIG. 4 (THESE DATA ARE AVERAGED OVER TEN DEVICES PER PROCESSING CONDITION)

Plasma condition	J_{sc} (mA·cm^{-2})	V_{oc} (V)	FF	PCE (%)
25 W/2 s	7.81 ± 0.24	0.55 ± 0.01	26.2 ± 1.68	1.12 ± 0.10
25 W/10 s	8.45 ± 0.58	0.56 ± 0.01	27.1 ± 0.36	1.29 ± 0.11
25 W/25 s	8.54 ± 0.44	0.57 ± 0.01	34.8 ± 1.74	1.70 ± 0.18
18 W/25 s	7.73 ± 0.14	0.56 ± 0.01	38.3 ± 2.25	1.65 ± 0.07
18 W/60 s	7.15 ± 0.07	0.57 ± 0.01	34.9 ± 3.85	1.42 ± 0.17

60 s, also demonstrated a slightly reduced PCE of 2.53%. The PCE is not sensitive to the treatment time at low plasma power. According to these results, we infer that the photoactive layer would be damaged by the high-power N_2 treatment. However, the degradation degree of the photoactive layer could be relatively reduced when using a low-power N_2 plasma treatment. We quantitatively demonstrate the plasma damage effect at the irradiation of high flux of nitrogen ions (25 W). However, the damage effect becomes very small at the irradiation of low flux of 18 W. It can be explained that the ionization rate is low enough to be offset by the self-curing rate at room temperature. This study demonstrates the critical point of plasma power (ionizing rate) to radiation damage at room temperature.

It can be deduced that the improvement of the surface wettability between the photoactive layer and PH1000 anode by N_2 plasma could enhance the PCE of fully spray-coated OPVs. Therefore, we spray-coated highly conductive PH1000 on the various plasma-modified photoactive layers to replace the conventional MoO_3/Ag as the top electrode. The previous literature [15] had pointed out that the transmittance and sheet resistance of PH1000 anode vary with the thickness. The optimum balance between transmittance and sheet resistance due to the tradeoff effect occurs at a certain thickness. For determining the optimum thickness of the semitransparent anode, we coated the PH1000 films with various thicknesses by a spraying process. The result shows that the spray-coated PH1000 film with a thickness of 2 μm (sprayed by 20 cycles) exhibits the optimum condition with the sheet resistance and transmittance of 20 $\Omega\cdot\square^{-1}$ and 20%, respectively. The transmittance curves corresponding to different thicknesses are shown in Fig. 3. The determined thickness agrees with the result of the previous study [15].

Based on the semitransparent PH1000 thickness fixed at 2 μm, we prepared the fully coated devices with the photoactive layers treated with 25 W of plasma for 2, 10, and 25 s, and 18 W of plasma for 25 and 60 s. The measured *J–V* curves are shown in Fig. 4. The corresponding device performance of these devices is listed in Table II. It is noteworthy that we cannot yield the available PCE of the device without plasma modification because the PH1000 solution spray-coated on the photoactive layer tends to shrink into some separated droplets and cannot form a continuous film due to the poor wettability. The PCE of devices treated with high-power (25 W) N_2 plasma for 2, 10, and 25 s was 1.12%, 1.29%, and 1.70%, respectively. The PCE was enhanced with increasing N_2 plasma-treated time. It implies that the N_2 plasma modification improves the surface wettability and facilitates the interfacial contact between the hydrophobic photoactive layer and hydrophilic PH1000 layer. In contrast to the degraded performance with increasing the plasma effect (shown by the devices with the evaporated MoO_3/Ag anode; Table I), we can conclude that the enhancement due to the improved wettability with increasing the plasma strength overcomes the induced-damage of the active layer. This result demonstrates that the net effect caused by the plasma treatment on PCE is positive. Moreover, we modified the fully sprayed devices with low-power (18 W) N_2 plasma for 25 and 60 s. The corresponding PCEs of these devices were 1.65% and 1.42%, respectively. The PCE of the device modified with low-power N_2 plasma for 25 s is similar to that treated with high-power N_2 plasma for 25 s. Interestingly, the fill factor of devices treated with low power N_2 plasma is better than that treated with high power N_2 plasma. These results provide the evidence that the N_2 plasma is a facile approach to fabricate fully spray-coated OPVs, although the PCE of fully spray-coated OPVs is still much lower than that of devices based on the evaporated electrodes. The lower PCE of fully spray-coated OPVs is closely related to the poor fill

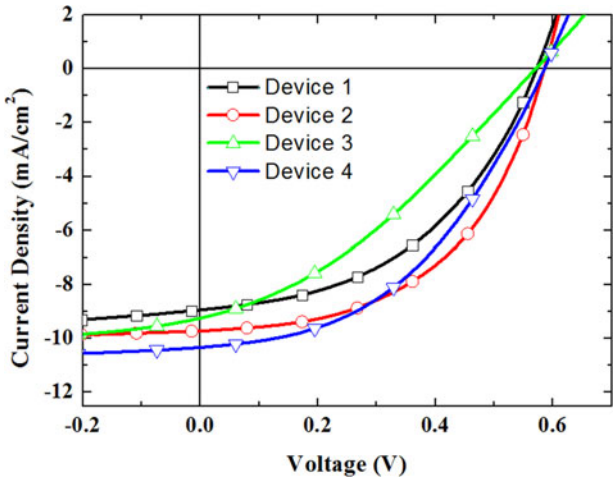

Fig. 5. Voltage–current characteristics of the spray-coated cell devices based on the evaporated MoO_3/Ag anode (device 1 and device 2) and the spray-coated PH1000 anode (device 3 and device 4). Devices 1 and 3 were only treated with pre-annealing at 130 °C for 10 min. Devices 2 and 4 were treated with the same pre-annealing plus the postannealing at 100 °C for 10 min.

factor, which implies the interfacial contact between the PH1000 and photoactive layer should be improved further. Because of the similar performance of devices treated with either high- or low-power N_2 plasma, we adopted the N_2 plasma power of 18 W for 25 s as the subsequently optimum parameters to fabricate fully spray-coated devices (in the following experiment) and also reduce the plasma damage as possible.

B. Thermal Treatment of the PH1000 Anode in the Fully Spray-Coated Cells and Modules for Performance Improvement

It has been demonstrated that the N_2 plasma modification can significantly enhance the performance from ∼0% to 1.70% due to the improving wettability or interfacial compatibility between photoactive and PH1000 layers. We subsequently heated or thermally cured the PH1000 layer after spray-coating it on the photoactive layer to 1) further improve the interfacial contact and 2) improve the inner structure of the PH1000 anode for reducing its sheet resistance. However, the previous photoactive layer was fabricated by the pre-annealing at 130 °C for 10 min for a proper phase separation of donor and acceptor materials to obtain a good performance (a good bulk heterojunction (BHJ) structure). We should clarify the effect of the extra thermal treatment (processing of the PH1000 anode at 100 °C for 10 min) on the photoactive layer first. For reference purposes, the spray-coated devices based on the evaporated MoO_3/Ag anode and the spray-coated PH1000 anode were tested with two kinds of treatments: 1) only pre-annealing at 130 °C for 10 min and 2) the pre-annealing plus postannealing at 100 °C for 10 min. Although the morphology evolution of the photoactive layer would be influenced by the top interface, we cannot avoid the additional thermal treatment during the devices manufacturing when we used a solution-processed top electrode. The reference devices based on the evaporated MoO_3/Ag anode are used to make sure that the additional thermal treatment would not affect the PCE of devices dramatically due to the deterioration of the P3HT:PCBM layer. Hence, we can clarify the impact of the solution-processed top electrode on the PCE of devices by excluding the damage to the active layer from the additional thermal treatment. The *J–V* characteristics of the prepared cell devices are shown in Fig. 5. The device performance and electric property are listed in Table III. The reference cell with the evaporated MoO_3 anode (device 1) only pre-annealed by 130 °C for 10 min showed J_{sc} of 8.99 mA · cm^{-2}, V_{oc} of 0.57 V, and FF of 54.2%, yielding a PCE of 2.79%. The device with the evaporated MoO_3 anode (device 2) treated with the pre-annealing plus postannealing (100 °C for 10 min) shows a slightly decreasing PCE of 2.92%. This result implies that the effect of the postanneal process on the active layer is almost negligible. The fully spray-coated device with the semitransparent PH1000 anode (device 3) only treated with pre-annealing has a PCE of 1.79%. Moreover, the fully spray-coated device with the semitransparent PH1000 anode (device 4) treated with the same pre-annealing plus postannealing showed J_{sc} of 10.39 mA · cm^{-2}, V_{oc} of 0.60 V, FF of 46.5%, and PCE of 2.90%. The PCE is dramatically improved from 1.79% to 2.90% mainly due to the significant enhancement in J_{sc} and FF. This result evidences that the charge transport vertically from the photoactive layer to the top electrode and transversely inside the top electrode is improved by the postanneal treatment of the PH1000 anode. Moreover, the series resistance (R_s) of the OPV device treated with the postanneal process is reduced from 41.62 to 20.04 Ω·cm^2. This reduction reveals that a good ohmic contact between the photoactive layer and spray-coated PH1000 layer is formed. In addition, the increase of shunt resistance (R_{sh}) from 203.28 to 596.44 Ω · cm^2 also implies that the postanneal process reduces the photocurrent leakage and charge recombination due to the improved interfacial contact.

TABLE III
PHOTOVOLTAIC PERFORMANCE AND ELECTRIC PROPERTY CORRESPONDING TO FIG. 5

Devices	J_{sc} (mA·cm^{-2})	V_{oc} (V)	FF (%)	PCE (%)	R_s (Ω·cm^2)	R_{sh} (Ω·cm^2)
1	8.99	0.57	54.2	2.79	19.65	432.51
2	9.72	0.59	51.3	2.92	11.58	894.68
3	9.27	0.57	33.8	1.79	41.62	203.28
4	10.39	0.60	46.5	2.90	20.04	596.44

In addition to the all-spray-coated cell devices, we up-scaled the cell technique of a module consisting of three cells (1 cm × 4 cm for each cell) connected in series by this process. The picture and the related *J–V* curves of the all-spray-coated module are shown in Fig. 6. The module presents V_{oc} of 1.689 V, J_{sc} of 3.22 mA · cm^{-2}, FF of 44.7%, and therefore a promising PCE of 2.44%. The PCE of this sprayed module is close to that of single devices. A similar performance between single devices and module implies that the semitransparent PH1000 could be utilized as an effectively alternative electrode in module due to a tiny connected loss.

The stability is an important issue toward commercialization. The stability tests of the unencapsulated spray-coated devices based on the evaporated MoO_3/Ag and the spray-coated

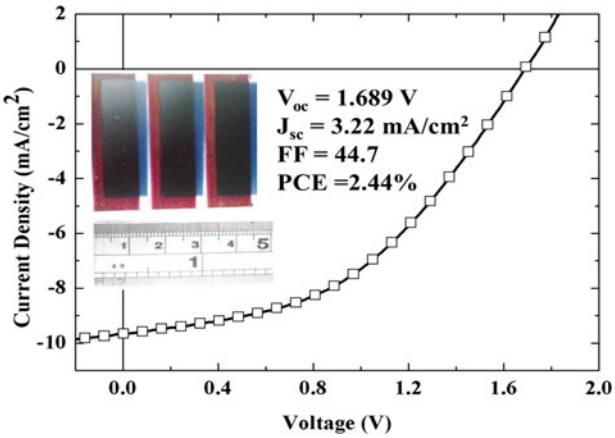

Fig. 6. Picture and the performance of the fully spray-coated module.

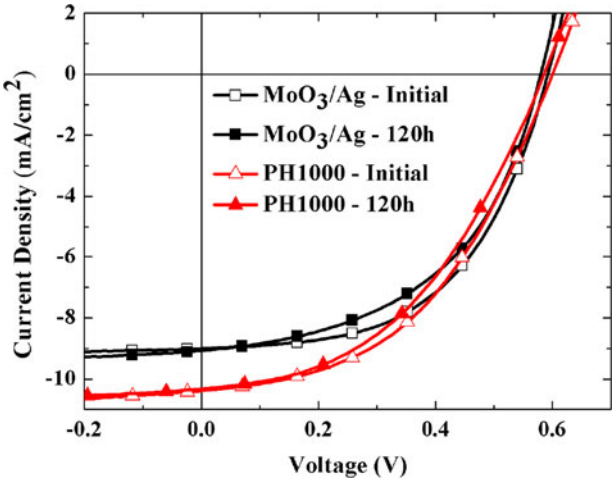

Fig. 7. Voltage–current characteristics of the spray-coated devices, which are stored in ambient environment for 120 h, based on the evaporated MoO_3/Ag anode and the spray-coated PH1000 anode.

TABLE IV
PHOTOVOLTAIC PERFORMANCE CORRESPONDING TO FIG. 7 (THESE DATA ARE AVERAGED OVER TEN DEVICES PER PROCESSING CONDITION)

HTL storage time	J_{sc} (mA·cm^{-2})	V_{oc} (V)	FF	PCE (%)
MoO_3 initial	9.29 ± 0.38	0.58 ± 0.01	51.27 ± 2.65	2.77 ± 0.23
MoO_3 120 h	9.1 ± 0.37	0.58 ± 0.01	52.98 ± 1.16	2.44 ± 0.30
PH1000 initial	10.56 ± 0.24	0.59 ± 0.01	42.85 ± 5.16	2.68 ± 0.30
PH1000 120 h	10.52 ± 0.25	0.58 ± 0.01	42.56 ± 3.25	2.58 ± 0.19

PH1000 top electrodes were performed using an ISOS-D-1 protocol (shelf, under air condition; stored in air for 120 h). The variations of *J–V* curves, V_{oc}, J_{sc}, FF, and PCE of the devices based on these two anodes before and after 120 h are shown in Fig. 7 and Table IV, respectively. According to the stability data, we can observe that there are no significant decay behaviors in the two devices. The fully sprayed devices showed a comparable stability to the devices with the thermally evaporated top electrode of MoO_3/Ag. This result implies again that the PH1000 is a good alternative electrode to the thermally evaporated electrode, and the solution-processed electrode is a more energy saving process than the thermally evaporated electrode.

IV. CONCLUSION

After improving the wettability by plasma modification, the PCE can be achieved to 1.70% because the positive effect of plasma-improved wettability overcomes the damage effect on the active layer. This study provides the optimum plasma parameters. Moreover, the improved PCE with the semitransparent electrode can be achieved to 2.90% by combining the further thermal annealing to remove the plasma-induced defects in the active layer. Compared to the fully spray-coated devices only treated with pre-annealing (PCE $\sim$ 1.79%), a much better shunt resistance was achieved by this approach, suggesting the reduction in the leakage current and recombination. Note that the PCE is the highest PCE among the fully sprayed inverted P3HT:PCBM devices with the semitransparent PH1000 anode currently reported in the literature. In summary, we fabricated all-solution cell and module devices by the spray process. The highly conductive PH1000 layer was used as the top semitransparent electrode to replace the metal electrode deposited by thermal evaporation. N_2 plasma treatment was developed here to improve the wettability between hydrophilic PH1000 and hydrophobic P3HT:PCBM layers. Furthermore, we demonstrated that the post-thermal treatment regarding the PH1000 electrode plus pre-annealing for the active layer is critical to the PCE of all-solution devices. The PCE of 2.90% and 2.44% for the all-sprayed cell and module devices was achieved, respectively. This facile external treatment paves a way to the modification of the photoactive layer, which is useful to the all-solution OPVs or a tandem junction solar cell.

REFERENCES

[1] Z. Wang *et al.*, "Polymer solar cells exceeding 10% efficiency enabled via a facile star-shaped molecular cathode interlayer with variable counterions," *Adv. Funct. Mater.*, vol. 26, pp. 4643–4652, 2016.
[2] D. Joly *et al.*, "Metal-free organic sensitizers with narrow absorption in the visible for solar cells exceeding 10% efficiency," *Energy Environ. Sci.*, vol. 8, pp. 2010–2018, 2015.
[3] S. Woo *et al.*, "8.9% Single-stack inverted polymer solar cells with electron-rich polymer nanolayer-modified inorganic electron-collecting buffer layers," *Adv. Energy Mater.*, vol. 4, 2014, Art. no. 1301692.
[4] J.-D. Chen *et al.*, "Single-junction polymer solar cells exceeding 10% power conversion efficiency," *Adv. Mater.*, vol. 27, pp. 1035–1041, 2014.
[5] R. Søndergaard, M. Hösel, D. Angmo, T. T. Larsen-Olsen, and F. C. Krebs, "Roll-to-roll fabrication of polymer solar cells," *Mater. Today*, vol. 15, pp. 36–49, 2012.
[6] Y.-C. Huang *et al.*, "Facile hot solvent vapor annealing for high performance polymer solar cell using spray process," *Sol. Energy Mater. Sol. Cells*, vol. 114, pp. 24–30, 2014.
[7] R. R. Søndergaard, M. Hösel, and F. C. Krebs, "Roll-to-roll fabrication of large area functional organic materials," *J. Polym. Sci. B, Polym. Phys.*, vol. 51, pp. 16–34, 2013.
[8] Y. Zhang, J. Griffin, N. W. Scarratt, T. Wang, and D. G. Lidzey, "High efficiency arrays of polymer solar cells fabricated by spray-coating in air," *Prog. Photovolt. Res. Appl.*, vol. 24, pp. 275–282, 2015.
[9] F. Wu *et al.*, "Morphology construction of vertical phase separation for large-area polymer solar cells," *Org. Electron.*, vol. 26, pp. 48–54, 2015.
[10] L.-M. Chen *et al.*, "Multi-source/component spray coating for polymer solar cells," *ACS Nano*, vol. 4, pp. 4744–4752, 2010.
[11] H.-Y. Park *et al.*, "Facile external treatment for efficient nanoscale morphology control of polymer solar cells using a gas-assisted spray method," *J. Mater. Chem.*, vol. 21, pp. 4457–4464, 2011.

[12] M.-H. Chen, Y.-C. Kuo, H.-H. Lin, Y.-P. Chao, and M.-S. Wong, "Highly stable inverted organic photovoltaics using aluminum-doped zinc oxide as electron transport layers," *J. Power Sources*, vol. 275, pp. 274–278, 2015.
[13] S. B. Darling and F. You, "The case for organic photovoltaics," *RSC Adv.*, vol. 3, pp. 17633–17648, 2013.
[14] Y.-J. Kang, D.-G. Kim, J.-K. Kim, W.-Y. Jin, and J.-W. Kang, "Progress towards fully spray-coated semitransparent inverted organic solar cells with a silver nanowire electrode," *Org. Electron.*, vol. 15, pp. 2173–2177, 2014.
[15] J.-W. Kang *et al.*, "All-spray-coated semitransparent inverted organic solar cells: From electron selective to anode layers," *Org. Electron.*, vol. 13, pp. 2940–2944, 2012.
[16] J.-W. Kang *et al.*, "Fully spray-coated inverted organic solar cells," *Sol. Energy Mater. Sol. Cells*, vol. 103, pp. 76–79, 2012.
[17] F. Guo *et al.*, "Fully printed organic tandem solar cells using solution-processed silver nanowires and opaque silver as charge collecting electrodes," *Energy Environ. Sci.*, vol. 8, pp. 1690–1697, 2015.
[18] F. Guo *et al.*, "Nanowire interconnects for printed large-area semitransparent organic photovoltaic modules," *Adv. Energy Mater.*, vol. 5, 2015, Art. no. 1401779.
[19] H. P. Kim, H. J. Lee, A. R. b. Mohd Yusoff, and J. Jang, "Semi-transparent organic inverted photovoltaic cells with solution processed top electrode," *Sol. Energy Mater. Sol. Cells*, vol. 108, pp. 38–43, 2013.
[20] Z. Ding, V. Stoichkov, M. Horie, E. Brousseau, and J. Kettle, "Spray coated silver nanowires as transparent electrodes in OPVs for building integrated photovoltaics applications," *Sol. Energy Mater. Sol. Cells*, vol. 157, pp. 305–311, 2016.
[21] Y.-C. Huang, H.-C. Cha, C.-Y. Chen, and C.-S. Tsao, "A universal roll-to-roll slot-die coating approach towards high-efficiency organic photovoltaics," *Prog. Photovolt.*, vol. 25, pp. 928–935, 2017. doi: 10.1002/pip.2907.
[22] S.-L. Lim *et al.*, "Efficient, large area organic photovoltaic modules with active layers processed with non-halogenated solvents in air," *Org. Electron.*, vol. 43, pp. 55–63, 2017.
[23] T. Zhang *et al.*, "Fabricating high performance polymer photovoltaic modules by creating large-scale uniform films," *Org. Electron.*, vol. 32, pp. 126–133, 2016.
[24] M. V. Srinivasan, N. Tsuda, P.-K. Shin, and S. Ochiai, "Performance evaluation of PTB7:PC_{71}BM based organic solar cells fabricated by spray coating method using chlorine free solvent," *RSC Adv.*, vol. 5, pp. 56262–56269, 2015.
[25] Y. Zhang, N. W. Scarratt, T. Wang, and D. G. Lidzey, "Fabricating high performance conventional and inverted polymer solar cells by spray coating in air," *Vacuum*, vol. 139, pp. 154–158, 2017.
[26] K. Takahira, A. Toda, K. Suzuki, and T. Fukuda, "Highly efficient organic photovoltaic cells fabricated by electrospray deposition using a non-halogenated solution," *Phys. Status Solidi A*, vol. 214, 2017, Art. no. 1600536.
[27] C. Cai *et al.*, "Polymer solar cells spray coated with non-halogenated solvents," *Sol. Energy Mater. Sol. Cells*, vol. 161, pp. 52–61, 2017.
[28] D. W. Clegg and A. A. Collyer, *Irradiation Effects on Polymers*, 1st ed. Dordrecht, The Netherlands: Springer, 1991.
[29] G. S. Was, *Fundamentals of Radiation Materials Science*, 1st ed. Berlin/Heidelberg, Germany: Springer-Verlag, 2010.
[30] N. Li *et al.*, "Towards large-scale production of solution-processed organic tandem modules based on ternary composites: Design of the intermediate layer, device optimization and laser based module processing," *Sol. Energy Mater. Sol. Cells*, vol. 120, pp. 701–708, 2014.

Authors' photographs and biographies not available at the time of publication.